Title
Strain evolution in non-stoichiometric heteroepitaxial thin-film perovskites

Journal
Journal of Materials Chemistry C, 1(48)

ISSN
2050-7526

Authors
Breckenfeld, E
Shah, AB
Martin, LW

Publication Date
2013

DOI
10.1039/c3tc31653j

Peer reviewed

Journal of Materials Chemistry C

RSC Publishing

PAPER

View Article Online
View Journal | View Issue

Cite this: J. Mater. Chem. C, 2013, 1, 8052

Strain evolution in non-stoichiometric heteroepitaxial thin-film perovskites†

E. Breckenfeld, A. B. Shah and L. W. Martin*

Epitaxial strain has been extensively used to control and induce new properties in complex oxide thin films. Understanding strain evolution and how to manipulate it are essential to the continued development of strain-induced effects in materials. The chemical complexity that underlies the diverse functionality of such oxide materials can have complex and unexpected effects on strain evolution and the breakdown of classic models of strain relaxation (*e.g.*, misfit dislocation formation). We explore the connection between the growth process and the diverse and extensive range of point and volumetric defects that can be generated and accommodated in oxide systems and how this ultimately impacts strain evolution. Pulsed-laser deposition was used to produce thin films of the prototypical perovskite oxide $SrTiO_3$ with chemical compositions ranging from 4% Sr-deficiency to 4% Sr-excess. Small variations in film composition are found to give rise to three distinct modes of strain relaxation, critical thicknesses for relaxation that vary from 60 to 300 nm, and have a notable impact on interfacial intermixing. Atomic-scale scanning transmission electron microscopy and spectroscopic studies provide information on defect structures, how the defect formations are connected to the epitaxial strain relaxation, and reveal that the presence of defect structures generally leads to a local chemical broadening of the interface.

Received 22nd August 2013
Accepted 24th October 2013

DOI: 10.1039/c3tc31653j

www.rsc.org/MaterialsC

Introduction

Thin-film heteroepitaxy has provided researchers with access to a range of novel functionalities across a multitude of material systems through lattice-induced misfit strain engineering. Such approaches have provided an opportunity to apply large biaxial strains (as large as several percent in some cases)[1,2] to nanoscale versions of materials which would lead to cracking in bulk versions of materials under similar values of hydrostatic strain. The ability to subject materials to such high strains without causing material failure has led to dramatic changes in the properties of materials including the enhancement of transition temperatures in ferroelectrics[3,4] and superconductors,[5] control of the nature of magnetism and magnetoresistance in colossal magnetoresistant materials,[6,7] manipulation of metal–insulator transitions in rare-earth nickelates,[8] and much more. Consequently, the control of strain has emerged as an important consideration when engineering structural, electronic, and magnetic properties in these systems.[9]

Despite great interest in the role of epitaxial strain on the evolution of properties in complex oxide thin films, quantitative understanding of strain evolution and relaxation remains underdeveloped. In traditional semiconductor systems, on the other hand, extensive work has revealed that strain accommodation is generally achieved by one of two mechanisms: (1) the breakdown of layer-by-layer growth and island formation[10] and (2) the nucleation of arrays of misfit or threading dislocations which break the coherence of the epitaxial interface.[11,12] Beyond experimental observations, modeling approaches have been developed that help to understand and predict the transition from elastic strain accommodation to plastic deformation and misfit dislocation nucleation in such systems. Classic approaches such as that of Frank and van der Merwe use energy minimization principles[13] and that of Matthews and Blakeslee use a force-balance approach[14] to predict the critical thickness for the formation of misfit dislocations. Both models are effectively equivalent when correctly formulated and predict identical critical thicknesses for systems such Si, Ge, and III–V semiconductor compounds.[12,15] Beyond these classic approaches, additional models have been developed that account for surface effects,[16] material anisotropy,[17] and to address the rare discrepancies found in such traditional systems.[18]

In general, the same deep understanding of strain relaxation is not available for complex oxide films. Although it is possible to observe similar strain relaxation mechanisms (*i.e.*, island formation and the formation of misfit dislocations arrays) in some oxide systems such as MgO,[19,20] $SrTiO_3$,[21–23] $BaTiO_3$,[24] and $LaAlO_3$,[25] other effects can also occur to drive

Department of Materials Science and Engineering and Materials Research Laboratory, University of Illinois, Urbana-Champaign, Urbana, IL 61801, USA. E-mail: lwmartin@illinois.edu; Tel: +1-217-244-9162

† Electronic supplementary information (ESI) available: Full details of the growth process, XPS and RBS studies, additional EELS studies, and reciprocal space mapping results are provided. See DOI: 10.1039/c3tc31653j

strain relaxation away from the classical predictions. In perovskite systems alone, it is possible to have strain-induced structural deformation including bond angle adjustments,[26] octahedral tilts,[27] the formation of ferroelastic domains,[28] and strain-induced phase transitions to structural polymorphs that possess structures with more favorable strain conditions.[29] To further complicate the situation, although much of the prior work on these topics (both experimental and theoretical) has assumed ideal stoichiometry for the films in question, recent studies have demonstrated that ideal stoichiometry is an exception, not a guarantee in many complex oxide systems grown by pulsed-laser deposition.[30–35] The effects of non-stoichiometry are exacerbated by the complex nature of defect structures in these materials and the ability of many complex oxides to accommodate large densities of point defects prior to forming secondary phases.[36] Such defect structures – including oxygen vacancy ordering – can dramatically impact the structure and properties of materials.[37,38] In $SrTiO_3$ for instance, where cation non-stoichiometry can arise as a function of laser fluence, growth pressure, deposition angle, and a range of other factors, researchers have demonstrated dramatic changes in the structure and properties (*i.e.*, electrical, thermal, and dielectric) with minor changes in the growth process.[30,31,39–42] It has even been suggested in passing that such non-stoichiometry-induced defects could play a role in film relaxation,[36,43] but a detailed understanding of the interplay between film composition, defect accommodation, and strain relaxation has not been undertaken.

With this in mind, we investigate the impact of cation non-stoichiometry on strain relaxation in a model perovskite thin-film system based on heteroepitaxial $SrTiO_3/NdGaO_3$ (110) films. We demonstrate that there is a strong link between film composition and strain relaxation behavior. In films possessing 4% Sr-excess the critical thickness for strain relaxation is ~60 nm and relaxation is not achieved by misfit dislocation formation, but by the formation of SrO interlayer structures that work to accommodate strain. In films possessing 4% Sr-deficiency, on the other hand, the critical thickness for strain relaxation is ~300 nm which is made possible by the inclusion of Sr-vacancies in the lattice which can help to accommodate strain until a critical thickness that is almost two orders-of-magnitude larger than that predicted by classical models. Finally, films possessing nearly-stoichiometric chemistry exhibit gradual relaxation between film thicknesses of 150–300 nm which is achieved by the gradual formation of misfit dislocations at the film-substrate interface. Additionally, it is observed that these defect structures also impact the atomic-scale precision of the heterointerface with the presence of point and line defects generally leading to a local chemical broadening of the interface. These results illustrate the necessity of carefully and systematically studying and controlling the chemistry and defect structures in complex oxide thin films and shed new light on additional reasons why oxide thin films do not generally follow classical models for strain relaxation. The implications of these observations for engineering strain in films are also discussed.

The lattice mismatch between $SrTiO_3$ and $NdGaO_3$ can be estimated by the equation $f_m = \frac{a - a_s}{a}$ (where a_s is the pseudo-cubic lattice constant of the $NdGaO_3$ substrate (3.86 Å) and a is the lattice constant of the $SrTiO_3$ film (3.905 Å)) to be −1.2% (compressive). According to the Matthews–Blakeslee model,[14] the critical thickness for film relaxation can be calculated based on the formula

$$h_c = \frac{(1 - \nu \cos^2\theta)b^2}{8\pi f(1+\nu)b_{\|}} \ln\left(\frac{\alpha h_c}{b}\right) \quad (1)$$

where b is the magnitude of the Burgers vector, $b_{\|}$ is the Burgers vector edge component parallel to the interface, f is the misfit strain, θ is the angle between the Burgers vector and the dislocation line of the misfit dislocation, ν is the average Poisson ratio of the film and substrate, and α is the cutoff radius of the dislocation core which is generally between 1 and 4.[24] Using the appropriate parameters for the $SrTiO_3/NdGaO_3$ (110) heterostructure[22] (b = 5.52, $b_{\|} = 3.905$, $f = -0.012$, $\nu = 0.25$, $\alpha = 1$, $\theta = 90°$) we calculate a critical thickness of only ~5 nm for this system.

Experimental

Thin films of $SrTiO_3$ with thicknesses between 30 nm and 330 nm were grown on $NdGaO_3$ (110) single crystal substrates using pulsed-laser deposition at a range of laser fluences using a KrF excimer laser (LPX 205, Coherent) at 750 °C in an oxygen pressure of 100 mTorr from a single crystal $SrTiO_3$ target (0.5 mm thick $SrTiO_3$ (001) single crystal, Crystec, GmbH). Films were grown on $NdGaO_3$ (110) single crystal substrates (with lattice parameters a = 0.543 nm, b = 0.550 nm, and c = 0.771 nm corresponding to a pseudocubic lattice parameter a_{pc} = 0.386 nm and a compressive lattice mismatch of 1.2% with the $SrTiO_3$). A laser spot size of 0.19 cm^2 was used for the growth of all films and by changing the laser energy the laser fluence was varied between 0.35 and 0.69 J cm^{-2}. Films grown at 0.35 J cm^{-2} were grown at 15 Hz and films grown at fluences in excess of 0.35 J cm^{-2} were grown at 5 Hz. The on-axis target-to-substrate distance was maintained at 6.35 cm for all depositions. Following the growth, the films were cooled at 5 °C min^{-1} to room temperature in 700 Torr of oxygen to promote oxidation. Additional details on the growth process are provided in the ESI† and in ref. 30.

Following growth, film stoichiometry was measured with X-ray photoelectron spectroscopy (Kratos Axis Ultra, XPS) and Rutherford backscattering spectrometry (RBS). Additional details are provided in the ESI (Fig. S1 and S2†) and in ref. 30. Structural studies were completed using high-resolution reciprocal space mapping X-ray diffraction studies (Panalytical, X′Pert MRD Pro, XRD). Cross-sectional electron microscopy studies were carried out in a 200 kV JEOL JEM2200FS aberration corrected scanning transmission electron microscope (STEM) coupled with electron energy loss spectroscopy (EELS). Specimens for electron microscopy were mechanically polished and ion milled at 3.5 kV followed by a final polish at 2.0 kV and 0.1 kV. Care was taken to reduce the ion beam current such that the milling rate was less than 2 μm per hour (additional details are provided in the ESI†).

Results and discussion

We begin by discussing the results of the chemical analysis of the films. XPS studies of the Sr 3d and Ti 2p core electron peaks (Fig. 1a), here shown after having the Tougaard background subtracted and normalized to the Sr-peak height, reveal clear differences in the Ti peak intensity consistent with deviations in film chemistry. Quantitative analysis of this data confirms the film stoichiometry for these three characteristic as-grown films to be 4% Sr-excess, nearly stoichiometric, and 4% Sr-deficient for films grown at laser fluences of 0.35 J cm^{-2}, 0.50 J cm^{-2}, and 0.69 J cm^{-2}, respectively. RBS experiments on these samples reveal the same compositions within ~1% error. It should be noted that conventional X-ray diffraction studies of these samples reveal no second phases and only minor shifts of the expected peak position for the $SrTiO_3$ films as a result of the chemical variations.

The strain state of all films (including both the in-plane and out-of-plane lattice parameters) was probed *via* X-ray reciprocal space mapping studies about the 103 and $0\bar{1}3$ diffraction conditions for the films and the 332 and 240 diffraction conditions of the substrate. Such analysis reveals three unique strain accommodation and relaxation processes that depend on the stoichiometry of the material (Fig. 1b and c). Films exhibiting Sr-excess are seen to be coherently strained only up to a critical thickness between 54 and 69 nm where relaxation occurs. The relaxation of both the in-plane (Fig. 1b) and out-of-plane (Fig. 1c) lattice parameter is rather sharp and in our study there are no films exhibiting intermediate lattice parameters between that of the $NdGaO_3$ substrate and the bulk $SrTiO_3$ value. Sr-deficient films show a similar sharp relaxation, but films remain coherently strained until relaxation occurs at a critical thickness of 280–300 nm. Note that films possessing both Sr-excess and Sr-deficiency relax to a value larger than the bulk $SrTiO_3$ lattice constant, consistent with prior studies that have shown an expansion of the lattice with non-stoichiometry. Nearly-stoichiometric films, on the other hand, behave quite differently. Films with a thickness of <150 nm are found to be coherently strained to the substrate. As the thickness increases beyond 150 nm, the films gradually relax until they are fully relaxed at a thickness of ~300 nm. It should be noted that the critical thickness for strain relaxation for all films is well in excess (1–2 orders-of-magnitude) of what is predicted from the Matthews–Blakeslee model for $SrTiO_3/NdGaO_3$. These results indicate that non-stoichiometry is either changing the energetics governing dislocation nucleation or providing alternate pathways for strain accommodation.

In order to understand the relaxation mechanisms and defect structures in these films, high-angle annular dark-field (HAADF) STEM imaging was used to probe films possessing Sr-excess, nearly-stoichiometric, and Sr-deficient chemistries. Because contrast in HAADF STEM scales with atomic number, our studies are most sensitive to the Sr ions in the film and the Nd ions in the substrate. Representative low-resolution HAADF images for films possessing Sr-excess (Fig. 2a), nearly-stoichiometric (Fig. 2b), and Sr-deficient (Fig. 2c) chemistries reveal stark differences. Here we discuss the observed defect structures and the implications for the evolution of strain relaxation.

Images of the samples possessing Sr-excess chemistries consistently reveal dark, ordered regions that are spread throughout the film thickness. These defect structures are essential to understanding the rapid strain relaxation that is achieved in these films. The STEM image shown here (Fig. 2a) is for a fully relaxed, 85 nm thick film. Upon close inspection, the first ~5 nm of the film appears to possess no defects, while the remainder of the film exhibits the presence of numerous regions of reduced brightness which manifest visibly as triangular patches (marked with white arrows). These dark regions are known to be planar faults of SrO (akin to what is observed in Ruddlesden Popper (RP) versions of this material).[44] Additionally, some of these patches contain dislocations where lattice bending causes additional reduced contrast. EELS analysis of these dark patches reveals significantly reduced signal intensity at the Ti-edge as would be expected from areas made up of SrO (ESI, Fig. S3†). These observations help to explain the relaxation behavior of the films possessing Sr-excess chemistry. The non-stoichiometry induced formation of these triangular and planar-like defect structures of SrO accommodate strain in a number of ways. First, they provide a site for the nucleation of misfit dislocations which can help to relax strain and it is

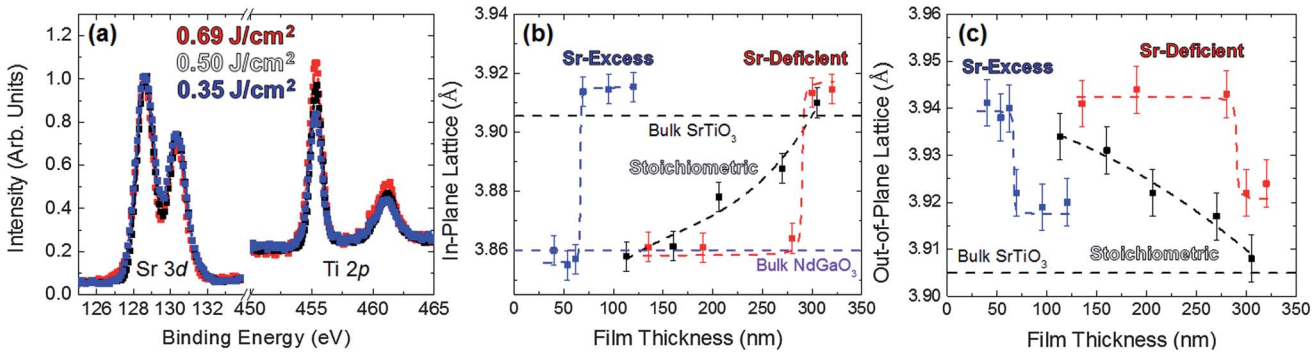

Fig. 1 (a) XPS spectra for various $SrTiO_3$ films where each spectra has had the Tougaard background subtracted and (for display purposes) the Sr 3d peak has been normalized to unity. (b) In-plane and (c) out-of-plane lattice parameter evolution for films grown to possess Sr-excess (blue), nearly-stoichiometric (black), and Sr-deficient (red) chemistries.

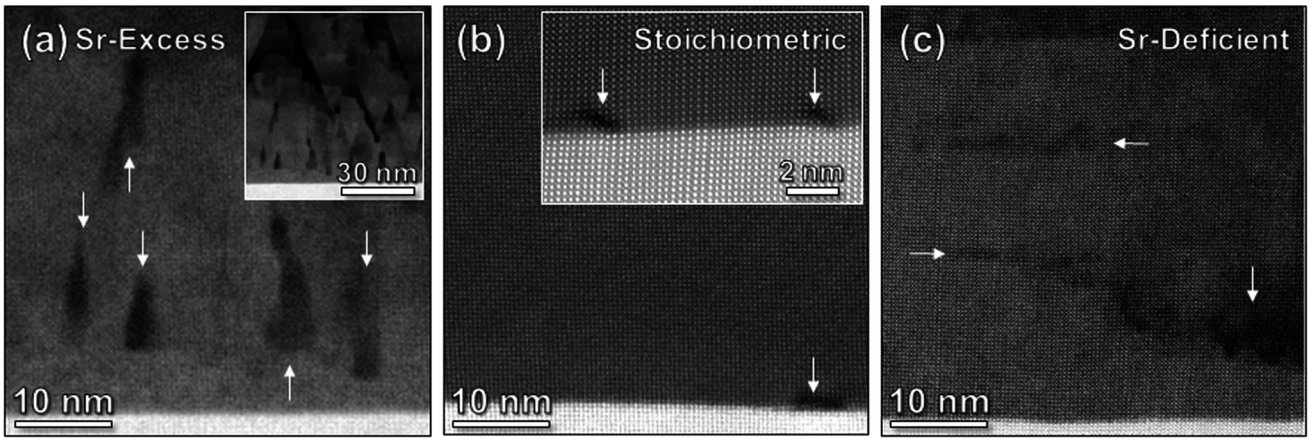

Fig. 2 Low-resolution scanning transmission electron microscopy images of $SrTiO_3$ films of various compositions. (a) Image of a film possessing Sr-excess where white arrows mark the location of SrO planar faults and the inset shows the changing distribution of these faults throughout the film thickness. (b) Image of a film possessing nearly ideal stoichiometry where misfit dislocations (marked with white arrows) form to gradually relax the strain. (c) Image of a film possessing Sr-deficiency where the white arrows mark areas of Sr-vacancy clustering.

known that terminating such SrO faults within a perovskite matrix can be accompanied by the formation of partial dislocations with a ½[111] Burgers vector. Second, the removal of a TiO_2 plane allows for contraction of the lattice within the plane-of-the-film which helps to accommodate the compressive strain imposed by the substrate. These observations are consistent with previous studies on $BaTiO_3$ where RP faults were found to provide a possible alternate pathway to strain relaxation.[43] The observation that there are no defects within the first 5 nm of the film is also interesting. To begin, this corresponds to the theoretical critical thickness for strain relaxation in this system. Although this could be a coincidence, one can image a scenario by which the growing film attempts to grow a coherently strained film by excluding excess Sr from the lattice (note that the presence of excess Sr has been shown to increase the lattice parameter of $SrTiO_3$ thereby further exacerbating the lattice mismatch) until a critical amount is obtained in the film and SrO planar-like faults are generated. These faults then propagate and serve as a sink for excess Sr and the equilibrium spacing of these features is impacted by the continuing strain evolution in the film (note the changing distribution of these regions with thickness in the inset of Fig. 2a).

The response observed in the nearly-stoichiometric films is quite different. Here we examine a relaxed 300 nm thick film (Fig. 2b). The nearly-stoichiometric films contain relatively sharp interfaces with periodic misfit dislocations (marked with white arrows) spaced by ~30 nm on average (although some closer spacings are observed, inset Fig. 2b). This spacing is close to the theoretically expected spacing of 32 nm that should arise as the dislocations accommodate the 1.2% lattice mismatch between film and substrate. Additionally, the bulk of the stoichiometric film shows even contrast, revealing no evidence of two- or three-dimensional defects away from the interface as expected. These observations help to explain the gradual relaxation trend observed with increasing film thickness in the nearly-stoichiometric films. As the film grows thicker, misfit dislocations are gradually nucleated to accommodate the growing strain energy. The critical thickness for complete strain relaxation of the $SrTiO_3$, however, is a factor of 60 greater than what would be predicted by the Matthews–Blakeslee model. Similar disconnects between predicted and experimentally observed critical thicknesses for perovskites have been observed previously.[22,24] These discrepancies are likely explained by the fact that the Mathews–Blakeslee estimation neglects a number factors important for complex oxides, including the fact that periodic surface steps common to the heterointerface of such oxide systems provide a resistance to the formation and motion of misfit dislocations,[16] that the Peierls–Nabarro stress due to electrostatic repulsion is expected to be much higher than that in covalent or metallic crystals which gives rise to a kinetic barrier to the introduction of dislocations, and that forces between second-nearest neighbors should not be neglected since in ionic crystals there is a strong repulsion between second-nearest neighbors of the same electronic charge.[22] In turn, these effects make it more difficult to nucleate a dislocation than is assumed in the Matthews–Blakeslee approach and thus strain relaxation is delayed until additional energy is built-up to initiate the process.

Unlike the other two compositions, the Sr-deficient films exhibit no evidence of misfit dislocation formation at the $SrTiO_3/NdGaO_3$ interface even in 250 nm thick films (Fig. 2c). Further away from the interface, however, slightly darker patches, which are believed to be vacancy clusters accommodating the Sr-deficiency, can be observed (marked with white arrows, Fig. 2c). Similar structures have been observed previously for Sr-deficient $SrTiO_3$ films, where they have also been attributed primarily to vacancy clusters.[35,44] These vacancy clusters appear to display some degree of ordering and could explain the strain accommodation and relaxation trends. Several works have demonstrated that point defects in $SrTiO_3$ are capable of screening epitaxial strain[45,46] by allowing small octahedral rotations and lattice contractions at second- or third-nearest-neighbor sites from the vacancy complexes. This seems to suppress the formation of misfit dislocations up to a certain

point (~300 nm in our study), after which sufficient strain energy has been built up so that dislocations can be formed and the strain is relaxed. These results have interesting implications for understanding relaxation mechanisms in oxide thin films. Taken together, these results indicate that the traditionally expected behavior (*i.e.*, misfit dislocation formation) will only occur in films that have no alternate mechanisms for strain relaxation.

Not only have we observed that the chemistry of the film can dramatically impact strain relaxation in these films, but additional EELS studies of the $SrTiO_3/NdGaO_3$ interface reveal a connection between the nature of interface precision and the chemistry and defect structures in the film. Interest in interfacial properties of materials has exploded in recent years[47,48] and with that comes concern about the precision and the control we can exert on the nature of heterointerfaces. Here we explore the role of nearby defects in mediating interface quality. It should be noted that in the pulsed-laser deposition process there are a number of potential driving forces for interfacial intermixing.[49] First, entropy alone can lead to intermixing in all interfacial systems, although the extent is highly dependent on the material system, the growth temperature, *etc.* Second, high-energy-adatoms, common to the pulsed-laser deposition process, can produce knock-on damage that can exacerbate intermixing. This effect is likewise dependent on the material, the temperature, the growth pressure, and the laser fluence used during deposition. Finally, electrostatic forces can cause intermixing at interfaces with polar discontinuities.[50] The interface between $SrTiO_3$ and $NdGaO_3$ is such an interface, as the substrate consists of alternating charged layers (NdO^+ and GaO_2^-) while the film consists of alternating neutral layers (SrO and TiO_2). In our work, the only factor which was varied between the different growths was the laser fluence which will give rise to changes in the adatom kinetic energy. For this reason, we can expect the entropic and electrostatic contributions to interfacial intermixing to be equal between different samples and for that reason we will not focus on those mechanisms here.

To probe the extent of intermixing, we employed scanning EELS studies across the interface. The half-width-at-half-maximum of the electron beam is ~2 Å and this sets the resolution limit for our studies. In this work, each reported line scan is the result of multiple line scans that were averaged to provide a picture of the interface chemistry. The EELS line scans were used to probe both the intensity of the Ti- and Nd-edges for films possessing Sr-excess (Fig. 3a), nearly-stoichiometric (Fig. 3b), and Sr-deficient (Fig. 3c) chemistries. For each film, we show the STEM image with white bars indicating the location of the line-scans. For the films possessing Sr-excess and nearly-stoichiometric chemistries, two scan types were performed: one at or near the location of a defect (*i.e.*, misfit dislocations for nearly-stoichiometric films and SrO planar-faults for the Sr-excess films) and one across an unperturbed portion of the interface. In the films with Sr-excess chemistry, we found varying degrees of chemical sharpness based on the location of the scan: 3–4 unit cells of intermixing near the location of a SrO planar-fault (Fig. 3a, line-scan 1) and 1–2 unit cells at the interface away form the SrO defects (Fig. 3a, line-scan 2). In the films with nearly-stoichiometric chemistry, we also found the extent of intermixing to be dependent on the scan location with intermixing extending 3–4 unit cells at or near a misfit dislocation (Fig. 3b, line-scan 1) and only 2–3 unit cells away from the misfit dislocations (Fig. 3b, line-scan 2). In the films possessing Sr-deficient chemistry, there were no major defects or dislocations found near the interface, and so only the unperturbed interface was scanned (Fig. 3c) and the intermixing was found to be confined to just 1–2 unit cells. The average interfacial width (as determined from both the Ti and Nd profiles) is summarized (Fig. 3d).

These results are somewhat counterintuitive with respect to laser fluence and adatom kinetic energy and indicate the impact of dislocations and defect structures on interfacial intermixing. The films possessing Sr-deficient chemistry exhibit the sharpest interfaces despite the fact that these films are grown at the highest laser fluence. Furthermore, the films possessing Sr-excess exhibit the largest extent of intermixing despite the fact that these films are grown with the lowest laser fluence. Empirically, one would expect the knock-on damage to scale with the laser fluence and thus the observed trends are counter to what might be expected. By considering the observed defect structures, however, the trends can be better understood. The films possessing Sr-deficient chemistries exhibit point defects clusters removed from the interface, but no misfit or volumetric defects in close proximity to the interface. Films possessing nearly-stoichiometric and Sr-excess chemistries exhibit periodic misfit dislocations and SrO planar-fault regions in close proximity (<5 nm) to the heterointerfaces. Both of these films exhibit, on average, more interfacial intermixing. The misfit dislocations and the SrO planar-faults appear to have similar effects and it is thought that the strain fields associated with these defects could promote interdiffusion and intermixing at the interface. This is consistent with prior observations of enhanced interdiffusion near misfit dislocations at the $PbZr_{0.52}Ti_{0.48}O_3/SrRuO_3$ heterointerface as a result of stress-assisted diffusion.[51] It is also possible that the local disruption of the electrostatics of the material (in the form of point, line, and volumetric defects that have charge associated with them) could give rise to additional driving forces for material diffusion and interaction.

Looking forward, these observations have a number of implications for controlling strain and relaxation in hetero-epitaxial oxide systems. By acknowledging and understanding the strong relationship between film composition and relaxation behavior/critical thickness one can envision routes by which researchers could greatly extend the magnitude of strain and the thickness of coherently strained films. From our studies, if one can simultaneously manipulate the lattice mismatch and gradually vary the composition and/or defect structure in a deterministic manner throughout the film thickness, one should be able to produce coherently strained films with greater thickness and larger overall strain values (without potentially diminishing the properties of the material). Not only does this have implications for potentially improved performance, but the study of films possessing compositionally and strain graded features could potentially open up new

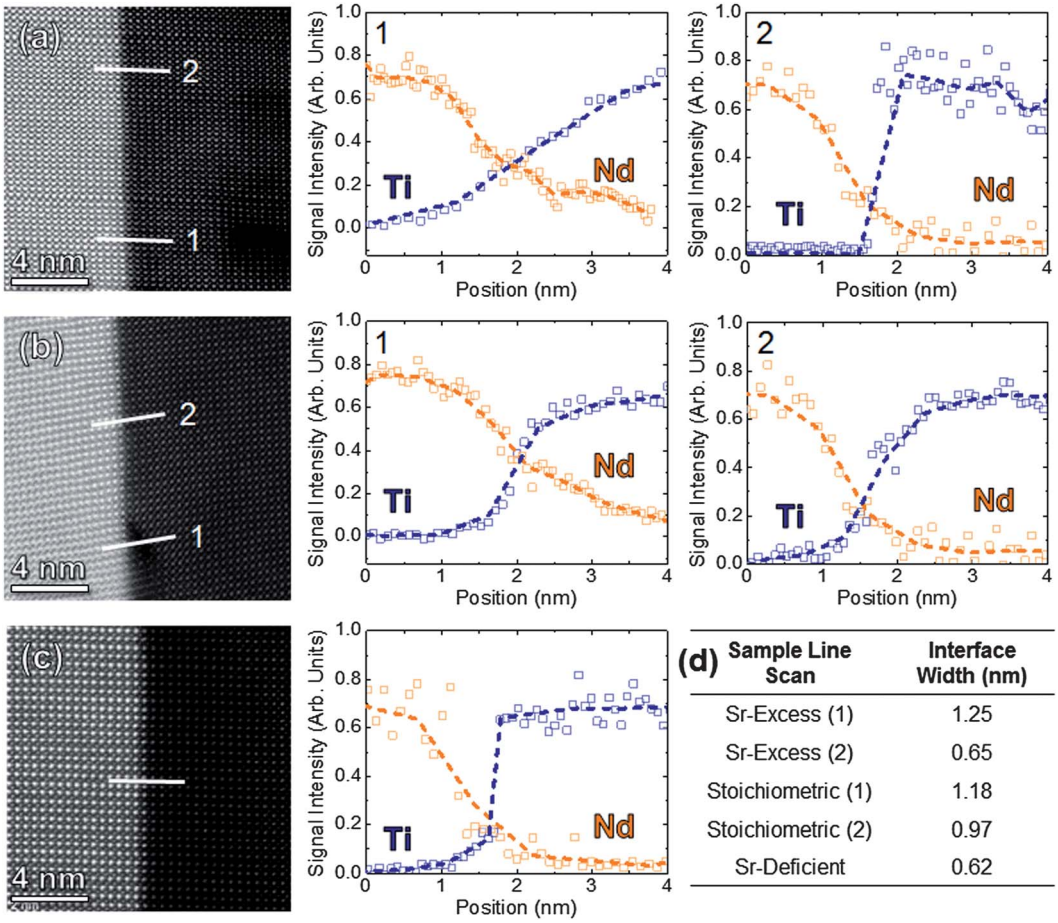

(d)

Sample Line Scan	Interface Width (nm)
Sr-Excess (1)	1.25
Sr-Excess (2)	0.65
Stoichiometric (1)	1.18
Stoichiometric (2)	0.97
Sr-Deficient	0.62

Fig. 3 Scanning EELS studies of interfacial intermixing at the $SrTiO_3/NdGaO_3$ (110) heterointerface. High-resolution STEM images and corresponding EELS line scans (white lines) for films possessing (a) Sr-excess, (b) nearly-stoichiometric, and (c) Sr-deficient chemistries. (d) Table summarizing the average interfacial width as determined from the EELS scans for both Nd and Ti.

realms of study.[52,53] This said, it should be noted that much remains to be understood about the precise mechanisms governing relaxation in such defective films and that not all of the measured non-stoichiometry in the films must necessarily be accommodated in the defect structures observed, but can also be accommodated *via* defects in the seemingly unperturbed areas (albeit in much lower concentrations). Overall advances in modern thin film growth, *in situ* characterization, and atomic-level control of complex oxides means that such defect engineering can potentially play an important role in a range of next generation applications and can potentially extend the realm of what is achievable.

Conclusions

In conclusions, in this work, we have induced changes in the stoichiometry of $SrTiO_3/NdGaO_3$ (110) films as a function of laser fluence during pulsed-laser deposition growth. By growing 4% Sr-excess, nearly-stoichiometric, and 4% Sr-deficient films, we have accessed a wide range of stoichiometry- and strain-accommodating defect structures. These defects were found to vary in type and the corresponding strain accommodation mechanism as a function of the film stoichiometry. We have shown strain relaxation *via* misfit dislocation formation to occur only in films with nearly ideal stoichiometry, but at thicknesses 1–2 orders-of-magnitude greater than that predicted by classical models. At the same time, films exhibiting both Sr-excess (*i.e.*, those with extended planar defects) and Sr-deficiency (*i.e.*, those with vacancy point defect clusters) experience alternate, lower energy mechanisms for strain relaxation and accommodation that leads to critical thicknesses for strain relaxation that vary from 60 nm to 300 nm. Furthermore, we observed the interfacial sharpness of these films – as evidenced by STEM EELS studies of interfacial intermixing – varies locally based on the relative proximity of such defect structures from 1 to 5 unit cells. Based on the defect structures we have observed and the connection to both strain relaxation and interfacial intermixing, we believe we demonstrated the importance of stoichiometry in truly understanding hetero-epitaxial strain relaxation processes in complex oxide systems. These results have broader implications for other oxide systems where epitaxial strain and interfacial intermixing are of concern and can dramatically impact the properties of those systems. These findings also help inform the deviation of complex oxide materials from more traditional models of strain relaxation. Until we can exert a more exacting level of compositional

control over these complex oxide system in our growth processes, we must understand all of the factors that might impact structural, strain, and property evolution.

Acknowledgements

The authors would like to acknowledge the help of R. Haasch and D. Jeffers for help performing the XPS and RBS studies, respectively. The work was supported by the National Science Foundation and the Nanoelectronics Research Initiative under grant DMR-1124696 and the U.S. Department of Energy under Grant DEFG02-07ER46459. Experiments were carried out in part in the Materials Research Laboratory Central Facilities.

Notes and references

1 D. G. Schlom, L.-Q. Chen, C.-B. Eom, K. M. Rabe, S. K. Streiffer and J. M. Triscone, *Annu. Rev. Mater. Res.*, 2007, **37**, 589.
2 L. W. Martin and D. G. Schlom, *Curr. Opin. Solid State Mater. Sci.*, 2012, **16**, 199.
3 K. J. Choi, M. Biegalski, Y. L. Li, A. Sharan, J. Schubert, R. Uecker, P. Reiche, Y. B. Chen, X. Q. Pan, V. Gopalan, L.-Q. Chen, D. G. Schlom and C.-B. Eom, *Science*, 2004, **306**, 1005.
4 J. H. Haeni, P. Irvin, W. Chang, R. Uecker, P. Reiche, Y. L. Li, S. Choudhury, W. Tian, M. E. Hawley, B. Craigo, A. K. Tagantsev, X. Q. Pan, S. K. Streiffer, L.-Q. Chen, S. W. Kirchoefer, J. Levy and D. G. Schlom, *Nature*, 2004, **430**, 758.
5 I. Bozovic, G. Logvenov, I. Belca, B. Narimbetov and I. Sveklo, *Phys. Rev. Lett.*, 2002, **89**, 107001.
6 A. J. Millis, T. Darling and A. J. Migliori, *J. Appl. Phys.*, 1998, **83**, 1588.
7 B. Raveau, A. Maignan, C. Martin and M. Hervieu, *Chem. Mater.*, 1998, **10**, 2641.
8 R. Scherwitzl, S. Gariglia, M. Gabay, P. Zubko, M. Gibert and J.-M. Triscone, *Phys. Rev. Lett.*, 2011, **106**, 246403.
9 D. G. Schlom, L.-Q. Chen, X. Q. Pan, A. Schmehl and M. A. Zurbuchen, *J. Am. Chem. Soc.*, 2008, **91**, 2429.
10 O. De Melo, C. Vargas-Hernandez and I. Hernandez-Calderon, *Appl. Phys. Lett.*, 2003, **82**, 43.
11 B. W. Dodson and J. Y. Tsao, *Appl. Phys. Lett.*, 1987, **51**, 1325.
12 J. Y. Tsao, B. W. Dodson, S. T. Picraux and D. M. Cornelison, *Phys. Rev. Lett.*, 1987, **59**, 2455.
13 F. C. Frank and J. H. van der Merwe, *Proc. – R. Soc. Edinburgh, Sect. A: Math. Phys. Sci.*, 1949, **198**, 216.
14 J. W. Matthews and A. E. J. Blakeslee, *J. Cryst. Growth*, 1974, **27**, 118.
15 P. M. J. Maree, J. C. Barbour and J. F. van der Veen, *J. Appl. Phys.*, 1987, **62**, 4413.
16 R. C. Cammarata and K. Sieradski, *Appl. Phys. Lett.*, 1989, **55**, 1197.
17 K. Shintani and K. Fujita, *J. Appl. Phys.*, 1994, **75**, 7842.
18 R. People and J. C. Bean, *Appl. Phys. Lett.*, 1985, **47**, 322.
19 F. Niu, A. L. Meier and B. W. Wessels, *J. Vac. Sci. Technol., B*, 2006, **24**, 2586.
20 Y. R. Li, X. Liang, Y. Zhang, J. Zhu, S. W. Jiang and X. H. Wei, *Thin Solid Films*, 2005, **489**, 245.
21 L. S.-J. Peng, X. X. Xi, B. H. Moeckly and S. P. Alpay, *Appl. Phys. Lett.*, 2003, **83**, 4592.
22 M. D. Biegalski, D. D. Fong, J. A. Eastman, P. H. Fuoss, S. K. Streiffer, T. Heeg, J. Schubert, W. Tian, C. T. Nelson, X. Q. Pan, M. E. Hawley, M. Bernhagen, P. Reiche, R. Uecker, S. Trolier-McKinstry and D. G. Schlom, *J. Appl. Phys.*, 2008, **104**, 114109.
23 Z. Y. Zhai, Z. S. Wu, H. L. Cai, X. M. Lu, J. H. Hao, J. Gao, W. S. Tan, Q. J. Jia, H. H. Wang and Y. Z. Wang, *J. Phys. D: Appl. Phys.*, 2009, **42**, 105307.
24 T. Suzuki, Y. Nishi and M. Fujimoto, *Philos. Mag. A*, 1999, **79**, 2461.
25 C. Merckling, M. El-Kazzi, G. Delhaye, V. Favre-Nicolin, Y. Robach, M. Gendry, G. Grenet, G. Saint-Girons and G. Hollinger, *J. Cryst. Growth*, 2007, **306**, 47.
26 A. Vailionis, H. Boschker, W. Siemons, E. P. Houwman, D. H. A. Blank, G. Rijnders and G. Koster, *Phys. Rev. B: Condens. Matter Mater. Phys.*, 2011, **83**, 064101.
27 F. Sandiumenge, J. Santiso, L. Balcells, Z. Konstantinovic, J. Roqueta, A. Pomar, J. P. Espinós and B. Martínez, *Phys. Rev. Lett.*, 2013, **110**, 107206.
28 K. Lee and S. Baik, *Annu. Rev. Mater. Res.*, 2006, **36**, 81.
29 A. R. Damodaran, C.-W. Liang, Q. He, C.-Y. Peng, L. Chang, Y.-H. Chu and L. W. Martin, *Adv. Mater.*, 2011, **23**, 3170.
30 E. Breckenfeld, R. W. Wilson, J. Karthik, A. R. Damodaran, D. G. Cahill and L. W. Martin, *Chem. Mater.*, 2012, **24**, 331.
31 T. Ohnishi, K. Shibuya, T. Yamamoto and M. Lippmaa, *J. Appl. Phys.*, 2008, **103**, 103703.
32 L. Qiao, T. C. Droubay, V. Shutthanandan, Z. Zhu, P. V. Sushko and S. A. Chambers, *J. Phys.: Condens. Matter*, 2010, **22**, 312201.
33 B. Dam, J. Rector, J. Johansson, J. Huijbregtse and D. De Groot, *J. Appl. Phys.*, 1998, **83**, 3386.
34 S. Wicklein, A. Sambri, S. Amoruso, X. Wang, R. Bruzzese, A. Koehl and R. Dittmann, *Appl. Phys. Lett.*, 2012, **101**, 131601.
35 D. Keeble, S. Wicklein, R. Dittmann, L. Ravelli, R. A. Mackie and W. Egger, *Phys. Rev. Lett.*, 2010, **105**, 226102.
36 T. Suzuki, Y. Nishi and M. Fujimoto, *Philos. Mag. A*, 2000, **80**, 621.
37 J. Gazquez, S. Bose, M. Sharma, M. A. Torija, S. J. Pennycook, C. Leighton and M. Varela, *Appl. Phys. Lett. Mater.*, 2013, **1**, 012105.
38 W. S. Choi, J.-H. Kwon, H. Jeen, J. E. Hamann-Borrero, A. Radi, S. Macke, R. Sutarto, F. He, G. A. Sawatzky, H. M. Kim and H.-N. Lee, *Nano Lett.*, 2012, **12**, 4966.
39 T. Hirano, M. Taga and T. Kobayashi, *Jpn. J. Appl. Phys.*, 1993, **32**, L1760.
40 M. Lippmaa, N. Nakagawa, M. Kawasaki, S. Ohashi and H. J. Koinuma, *J. Electroceram.*, 2000, **4**, 365.
41 T. Ohnishi, M. Lippmaa, T. Yamamoto, S. Meguro and H. J. Koinuma, *Appl. Phys. Lett.*, 2005, **87**, 241919.

42 D.-W. Oh, J. Ravichandran, C.-W. Liang, W. Siemons, B. Jalan, C. M. Brooks, M. Huijben, D. G. Schlom, S. Stemmer, L. W. Martin, A. Majumdar, R. Ramesh and D. G. Cahill, *Appl. Phys. Lett.*, 2011, **98**, 221904.
43 T. Suzuki, Y. Nishi and M. Fujimoto, *J. Am. Ceram. Soc.*, 2000, **83**, 3185.
44 C. M. Brooks, L. F. Kourkoutis, T. Heeg, J. Schubert, D. A. Muller and D. G. Schlom, *Appl. Phys. Lett.*, 2009, **94**, 162905.
45 D. A. Freedman, D. Roundy and T. A. Arias, *Phys. Rev. B: Condens. Matter Mater. Phys.*, 2009, **80**, 064108.
46 Y. Kim, A. S. Disa, T. E. Babakol and J. D. Brock, *Appl. Phys. Lett.*, 2010, **96**, 251901.
47 J. Chakhalian, A. J. Millis and J. Rondinelli, *Nat. Mater.*, 2012, **11**, 92.
48 H. Y. Hwang, Y. Iwasa, M. Kawasaki, B. Keimer, N. Nagaosa and Y. Tokura, *Nat. Mater.*, 2012, **11**, 103.
49 W. S. Choi, C. M. Rouleau, S. S. A. Seo, Z. Luo, H. Zhou, T. T. Fister, J. A. Eastman, P. H. Fuoss, D. D. Fong, J. Z. Tischler, G. Eres, M. F. Chisholm and H.-N. Lee, *Adv. Mater.*, 2012, **24**, 6423.
50 N. Nakagawa, H. Y. Hwang and D. A. Muller, *Nat. Mater.*, 2006, **5**, 204.
51 M. Arredondo, Q. M. Ramasse, M. Weyland, R. Mahjoub, I. Vrejoiu, D. Hesse, N. D. Browning, M. Alexe, P. Monroe and V. Nagarajan, *Adv. Mater.*, 2010, **22**, 2430.
52 R. V. K. Mangalam, J. Karthik, A. R. Damodaran, J. C. Agar and L. W. Martin, *Adv. Mater.*, 2013, **25**, 1761.
53 J. Karthik, R. V. K. Mangalam, J. C. Agar and L. W. Martin, *Phys. Rev. B: Condens. Matter Mater. Phys.*, 2013, **87**, 024111.